Chapter 2

Turbulence and Similarity Theory in Meteorology and Engineering

F.T.M. Nieuwstadt

J.M. Burgers Centre, Lab. Aero and Hydrodynamics
Technical University Delft, the Netherlands

Abstract

Due to lack of a definite theory, scaling is used in most cases to describe turbulent flows within a generalized frame work. This approach has been applied also with much success to the case of atmospheric turbulence. Here, we give a review of the various scaling approaches that have been developed for various regions and for various stability conditions in the dry atmospheric boundary layer. Where possible we have compared the scaling found in the atmosphere with the results found in the laboratory for engineering flows.

1 Introduction

In general terms a boundary layer is a thin layer adjacent to a surface in a flow at high Reynolds numbers. Across this layer the flow adjusts from the boundary condition at the surface to the flow conditions outside the boundary layer. In engineering applications one encounters such boundary layer over any object that moves in a fluid. Examples are an airplane, ship or a car. In the atmosphere, the term boundary layer is used with more or less a similar meaning. Here, it is the layer, which is thin with respect to the thickness of the total atmosphere and across which meteorological variables, such as wind velocity, temperature and humidity, adjust from their values in the free-atmosphere to their boundary conditions at the earth's surface.

Both in engineering and in the meteorology one wants to understand the flow process in the boundary layer in order to predict the transport of various variables. In the engineering examples mentioned above, this is mostly

the transport of momentum which when integrated over the whole surface results in one of the contributions to the drag of the moving object. In the atmosphere one is, apart from the momentum transport, usually also interested in the vertical transport of heat and humidity. These transport processes determine the fluxes of momentum, heat and humidity from the surface into the free atmosphere and these fluxes are among the major forcing terms for all atmospheric motions.

The fluxes of the meteorological variables mentioned above are directly responsible for the vertical profiles of these variables. It will be clear that these profiles will depend strongly on the process that determines vertical transport in the atmospheric boundary layer. This process is in general turbulence. Therefore, the study of the atmospheric boundary layer is almost synonym with a study of atmospheric turbulence. In this respect the study of atmospheric boundary layer is again close to engineering fluid mechanics where the flow is usually also turbulent. In engineering one has applied the notions of similarity theory and dimensions analysis for a long time and with much success. Therefore, it seems reasonable to expect that the same approach may be also fruitful for the study of atmospheric turbulence.

In a similarity or scaling approach one tries to identify scaling regimes of the atmospheric boundary layer. In each of these scaling regimes some physical process usually dominates. This allows us in many cases to introduce some simplifications or approximations in our description of the boundary layer. One of these simplifications is that we can distinguish so-called prototypes, which are representative for the boundary layer under some particular meteorological condition. These prototypes, which we shall discuss in some detail in the following sections, are: the surface layer, the neutral boundary layer, the convective boundary layer and the stable boundary layer. Our discussion is limited to the so-called dry boundary layer, i.e. we shall disregard the influence of condensation and evaporation on boundary-layer dynamics. Moreover, we shall also limit ourselves to a so-called horizontally homogeneous conditions which means that there is no variation of turbulence statistics in the horizontal direction.

We should mention here that although the similarity approach in engineering has a long tradition, its application to turbulence in the atmospheric boundary layer has developed only over the last decades. Nevertheless it has been very successful in describing several aspects of the horizontally homogeneous boundary layer under various conditions. The results of this scaling approach for the structure and the dynamics of the atmospheric boundary layer has been described in various textbooks (Stull, 1988; Arya, 1988; Garratt, 1992) and also in various review articles (Wyngaard, 1988; Wyngaard, 1992; Nieuwstadt, 1995; Nieuwstadt and Duynkerke, 1996). In this chapter we will give an overview of scaling in the atmospheric boundary layer where we aim in particular to concentrate on the similarities and differences of scaling in the atmosphere with scaling in engineering. We ask ourselves the question: is turbulence in engineering and in the atmosphere similar? This is an inter-

esting and important question to be answered in view of the fact that in the atmospheric boundary layer the Reynolds number is in general much larger than in engineering applications.

2 Similarity Theory

2.1 Atmospheric Turbulence

In this section we consider the processes that determine atmospheric turbulence and based on which we can apply scaling. Scaling can be interpreted as a selection of a region in parameter space where the boundary-layer structure or its dynamics is dominated by only a few (preferably a single) physical process(es), i.e. few compared to the total number of processes that can play a role in the boundary layer. This fact implies that variables can be scaled in terms of these dominating processes only or rather in terms of the scaling parameters by which these processes can be characterized. In most cases this permits us to derive simplified expressions for the various meteorological variables. Before we can discuss the various scalings of the atmospheric boundary layer we must first introduce the main scaling parameters.

As stressed above, scaling parameters must characterize physical processes. One of these is the consequence of no-slip boundary condition for the velocity at the surface. As a result the velocity must vary as a function of height and under the conditions that exist in the atmosphere, such velocity variation or velocity shear is unstable and consequently produces turbulence. This production process of turbulence is generally known as shear production. As parameter to characterize this process, we select the shear stress that the atmosphere experiences at the surface. This shear stress is denoted as τ_o from which we can obtain a velocity scale u_*, defined as

$$u_* = \sqrt{\frac{\tau_o}{\rho}} \,, \tag{1}$$

where ρ is the density of the air. This velocity scale is known as the friction velocity. It (or τ_o itself) can be used to characterize turbulence due to shear production in the boundary layer.

Another process that determines turbulence in the atmospheric boundary layer, is so-called buoyancy production. This process is related to motion of fluid elements with a different density than their surrounding due to the acceleration of gravity g. These density variations are in the atmospheric boundary layer the result of the temperature fluctuations which result from a heat flux imposed at the surface, H_o expressed in [W/m^2]. Let us first consider a pos-

itive heat flux, i.e. heat is introduced in the boundary layer at the surface. This heat flux will cause an increase in temperature near the surface or alternatively a decrease in density. Due to the acceleration of gravity this less dense air will tend to rise. For the conditions found in the atmosphere, this process is unstable and turbulence is generated. The other case is a negative surface heat flux, i.e. heat is removed from the boundary layer. The air near the surface will then be cooled and consequently its density increases. This situation is characterized as stable because the heavy air will resist vertical motion. As a result turbulence motion is opposed and in that case one would rather speak of buoyant destruction.

It is clear the buoyant production or destruction is characterized by the surface heat flux H_o. However, a more convenient scaling parameter is the surface temperature flux which is related to H_o according to $\overline{w'\theta'}_o = H_o/\rho c_p$ where c_p is the specific heat of air at constant pressure. The overbar indicates that we are considering a mean value and the prime denotes a (turbulent) fluctuation. Based on the temperature flux $\overline{w'\theta'}_o$, we can also define a temperature scale θ_* which is defined as $\theta_* = -\overline{w'\theta'}_o/u_*$. With help of the parameters u_* and θ_* we can define a length scale L given by

$$L = \frac{u_*^2}{k\frac{g}{T_o}\theta_*} , \tag{2}$$

where T_o (K) is the absolute temperature of the boundary layer (the combination g/T_o is sometimes denoted as the buoyancy parameter because it describes the vertical acceleration caused by a temperature fluctuation of 1 K). The k is a constant known as the Von-Karman constant which will be discussed in more detail below. The L given by (2) is called the Obukhov length scale. It can be interpreted as the height above the surface where buoyancy production starts to dominate over shear production. This interpretation will become clear in section 3.2 where we introduce the dimensionless ratio z/L where z is the height above the surface.

In view of our finding of a length scale as parameter to describe the relative importance of the two production processes of atmospheric turbulence, it seems useful to search for other length scales. It is a fact that the macro structure of turbulence scales with the geometry in which turbulence occurs. In our case this geometry can be characterized by δ which is defined as the depth of the turbulent layer above the surface and is called the boundary-layer height. Here we have used for this characteristic length scale the notation which is commonly used in engineering flows. The notation in atmospheric applications for the boundary-layer height is usually either h or z_i. The latter notation makes clear that the boundary-layer height is frequently connected to the height of an elevated temperature inversion.

If one considers the structure of the boundary layer it is clear that the height z above the surface must also play a role. With the other two length

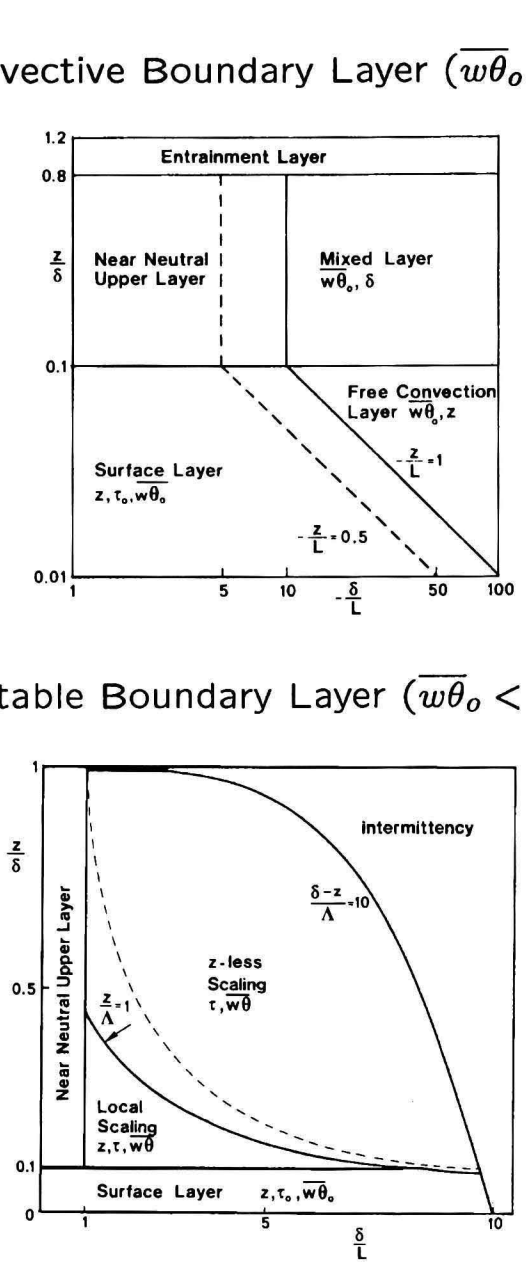

Fig. 1. Scaling regions in the convective ($\overline{w'\theta'}_o > 0$) and stable ($\overline{w'\theta'}_o < 0$) boundary layer; the lines denote the boundaries between the various scaling regimes (after Holtslag and Nieuwstadt, 1986).

scales introduced above we can now define two dimensionless combinations. These are z/δ and δ/L. The parameter z/δ gives the location in the boundary layer. The region near the surface, i.e. $z/\delta \leq 0.1$, is usually denoted as the surface layer. The parameter δ/L can be interpreted as a stability parameter which gives the relative importance of buoyancy production with respect

to shear production within the boundary layer. A values of $\delta/L < 0$ implies $\overline{w'\theta'}_o > 0$ so that buoyancy produces turbulence. For the case that this production process dominates (i.e. $-\delta/L \gg 1$) we call the boundary layer convective. When $\delta/L > 0$ or $\overline{w'\theta'}_o < 0$ buoyancy destroys turbulence and we call the boundary layer stable. For a value of δ/L around zero density effects will have small influence on the structure and dynamics of the boundary layer. This case is identified as a neutral boundary layer.

We can use both ratios δ/L and z/δ to define scaling regimes in the boundary layer. These scaling regimes are illustrated in Figure 1, after Holtslag and Nieuwstadt(1986). The scaling regimes can be interpreted as regions where boundary-layer turbulence can be typified in terms of a limited number of parameters. However, the scaling parameters introduced above are not always sufficient to describe all conditions or processes in the atmospheric boundary layer. For instance horizontal variation in the boundary conditions such as for the surface heat flux, requires an additional length scale. Description of the surface characteristics requires also a length scale for which the roughness length z_o is usually taken.

2.2 Comparison with Engineering Turbulence

In order to compare results obtained in the atmospheric boundary layer with results obtained in engineering flows we must use parameters which can be defined for both cases. The flow conditions in an engineering boundary layer are usually characterized by the Reynolds number $Re_m = U_e\delta_m/\nu$.
Here, δ_m is the momentum thickness which is defined as

$$\delta_m = \int_0^{\delta} \frac{u}{U_e}\left(1 - \frac{u}{U_e}\right) dz \ , \tag{3}$$

where δ is the boundary-layer thickness. The U_e is the velocity at the outer edge of the boundary layer.

Let us approximate the velocity profile by a logarithmic profile throughout the boundary layer:

$$u = \frac{U_e}{\ln(\delta/z_o)} \ln\left(\frac{z}{z_o}\right) \ ,$$

which satisfies the boundary conditions near the surface, i.e. $z \rightarrow z_o$ and at the top of the boundary layer: $\overline{u} = U_e$ at $z = \delta$. In that case the δ_m becomes equal to

$$\delta_m = \frac{\delta}{\ln(\delta/z_o)}\left(1 - \frac{2}{\ln(\delta/z_o)}\right) + \mathrm{O}\left(\frac{z_o}{\delta}\right) \ . \tag{4}$$

For boundary-layer heights found in the atmosphere which vary between 100 m and 1000 m and for a typical velocity of $U_e = 10$ m/s, we find with help of (4) that the Re_m varies between $\simeq 10^6$ and 10^7. These values for Re_m should be used when comparing scaling results with engineering data.

In the following sections we shall consider the scaling of the atmospheric boundary layer. We limit ourselves to the horizontally homogeneous boundary layer, i.e. a boundary layer without any horizontal variation so that profiles are only a function of height. Our treatment will be organized according to the prototypes of the boundary layer that we have mentioned in the introduction. For each case we consider the characteristic scaling parameters and illustrate how we can use them to formulate expressions for various boundary-layer variables. Where appropriate we will compare the atmospheric scaling results with engineering data for similar flow conditions.

3 Surface Layer Velocity Profiles

The surface layer is the region of the boundary layer close to the surface which is generally taken to be $z/\delta < 0.1$. The main simplification in the background for this is that the boundary-layer height δ is assumed to be no longer representative as estimate for the length scale of turbulence near the surface. As a consequence of its closeness to the surface, experiments in the surface layer can be carried out fairly easily. As a result much experimental data are available for the atmospheric surface layer which allows a detailed comparison of the atmospheric surface layer with engineering data.

In the following subsections we consider the consequences of the simplification that we have introduced for the scaling of the surface layer. We distinguish between a neutral surface layer, i.e. a surface layer without buoyancy production, and the diabatic surface layer where buoyancy effects are included. First we consider the mean velocity and temperature profiles and next the scaling of various turbulence statistics.

3.1 Neutral surface layer

In view of the fact that the boundary-layer height δ can be omitted as scaling parameters, the only length scales that remain in the neutral surface layer are: the height above the surface z and the roughness length z_o. The u_* remains of course as the appropriate scale for the velocity. This leads to the following scaling result for velocity profile

$$\frac{u}{u_*} = f\left(\frac{z}{z_o}\right) , \tag{5}$$

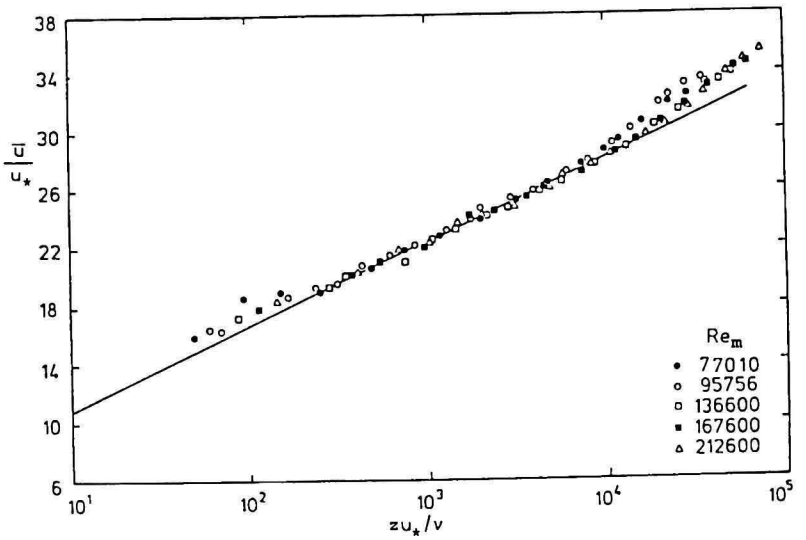

Fig. 2. The logarithmic profile observed in various engineering boundary layers at high values of the Reynolds number; the drawn line is given by (7) with $k = 0.4$ (Winter and Gaudet, 1973).

which in engineering terminology this is called the law of the wall. It has been verified for a large number of flows that (5) is indeed valid and for a review we refer e.g. to Monin and Yaglon (1971).

It is also well established that matching of (5) with the scaling relationship valid in the so-called outer layer of the boundary layer (to be discussed in section 5), leads to a logarithmic velocity profile in the overlap region between the two scaling regions. This logarithmic profile reads

$$u = \frac{u_*}{k} \ln\left(\frac{z}{z_o}\right) , \tag{6}$$

where k is known as the von-Karman constant for which one in general takes the value $k = 0.4$ (see e.g. Hinze, 1975).

For the case of an aerodynamically smooth surface $z_0 = 0.135\nu/u_*$ so that (6) becomes

$$u = \frac{u_*}{k} \left[\ln\left(\frac{zu_*}{\nu}\right) + 2.0\right] . \tag{7}$$

This equation has been frequently verified in engineering flows. Examples are shown in Figure 2 en 3 where we notice that in the last case the von-Karman constant is found to be considerably different from the accepted value mentioned above. The fact that one finds a different von-Karman constant which presumably is a universal constant, suggests that the "law of the wall" scaling

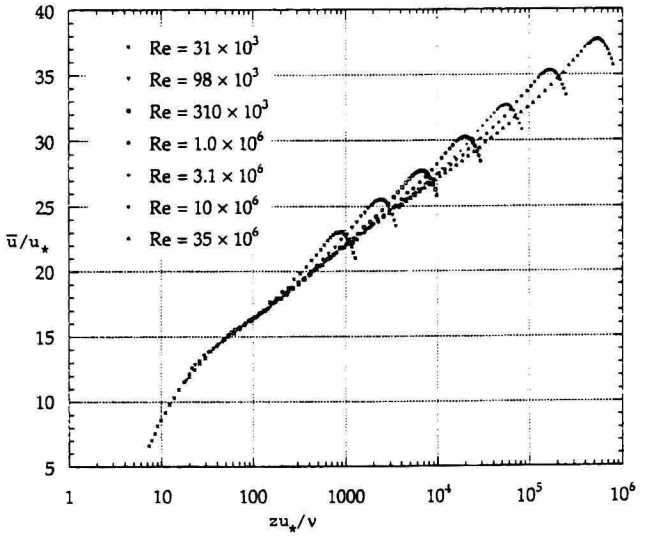

Fig. 3. The velocity profile observed in a pipe flow at high values of the Reynolds number where the Reynolds number in this case is defined as $u_* D/\nu$ with D the pipe diameter (Zagarola, 1996). The $u_* D/\nu$ can in this case be rewritten in terms of Re_m with help of (4) by inserting $\delta = D/2$. Fitting the logarithmic velocity profile to these data leads to $k = 0.435$.

and the resulting logarithmic velocity profile may not be as well established as it seems (Barenblat, 1993).

A boundary layer over an aerodynamically smooth surface in the atmosphere is the exception rather than the rule, in particular over land. However, recently some measurements were performed over a smooth salt flat (Folz, 1997). The resulting velocity profile under neutral conditions is shown in Figure 4. We find that the observations are slightly larger than by using (7) with $k = 0.4$. Most probably this is due to errors in the estimate of u_* which in this case was obtained by linear extrapolation of the velocity measured at the lowest observation height to zero at the surface. Nevertheless these results are a definite confirmation that over a smooth surface the velocity profiles in engineering and atmospheric boundary layers are similar.

As stressed above, a land surface can be almost always characterized as fully rough. As one of the consequences it has been proposed by Frenzen and Vogel (1995) that the value of the Von-Karman constant depends on the roughness. However, this would be in contradiction with the scaling assumption of an inner and outer layer which underlies the existence of the logarithmic velocity profile as argued below.

Our knowledge of turbulence above a rough surface is much less than over a smooth surface. Only little laboratory data on engineering flows over rough surface are available especially for cases representative for the atmospheric conditions. Here, we shall limit ourselves to discussion of only the

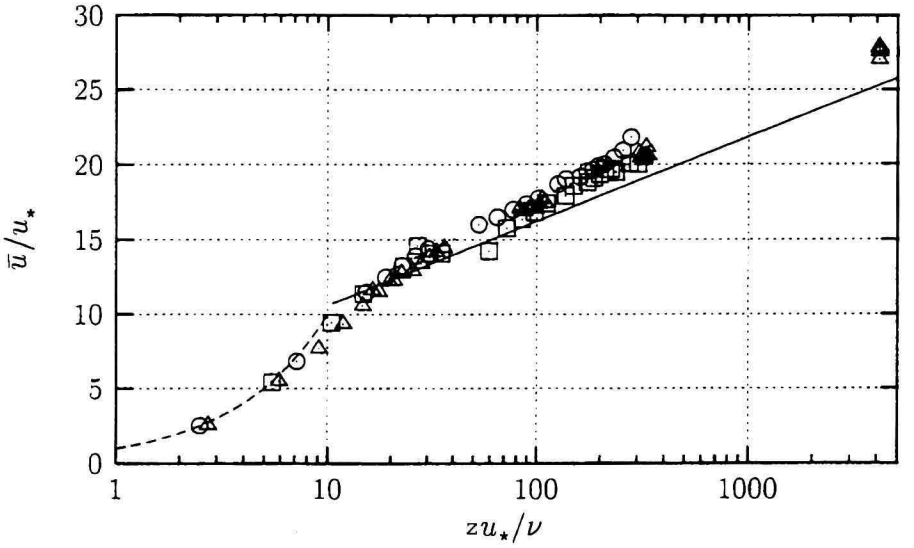

Fig. 4. The logarithmic profile observed in a atmospheric surface layer above a salt flat under neutral conditions; the solid line is the logarithmic profile with $k = 0.4$ and the dashed line is the linear profile valid in the viscous sublayer (Folz, 1997).

main aspects of rough surfaces and for a more extensive review we refer to Raupach et al. (1991).

The most common approach to treat the flow above rough surfaces is to assume that the details of the roughness only affect turbulence in the surface layer and not in the layer above. This implies that the "law of the wall" (5) should be extended with various additional variables which characterize the roughness. For the case of isolated roughness elements on a flat surface, these are for instance the height of the individual roughness elements (h) and their horizontal distribution which is usually described as the frontal area of an element per horizontal area (λ). For the case of vegetation one usually introduces λ as the leaf area index which is the cumulative leaf area per unit ground area.

Another complication is the fact that the origin of the z coordinate in (5) can no longer be taken at surface level $z = 0$. Instead one introduces a displacement height d which is the mean height of momentum absorption by the rough surface with for a smooth surface $d = 0$ and for a rough surface with $\lambda \to \infty$ the $d = h$. Let us assume that the matching procedure between the surface layer and the outer layer remains valid. This again results into a logarithmic profile given in this case by

$$\frac{u}{u_*} = \frac{1}{k} \ln\left(\frac{u_*(z-d)}{\nu}\right) - \left\{\frac{1}{k} \ln\left(\frac{u_* z_o}{\nu}\right) + \frac{\Delta_u\,(hu_*/\nu, \lambda)}{u_*}\right\} . \qquad (8)$$

The Δ_u is called the roughness function. This function is illustrated in Fig. 5 for various cases including laboratory experiments. We find that the Δ_u/u_*

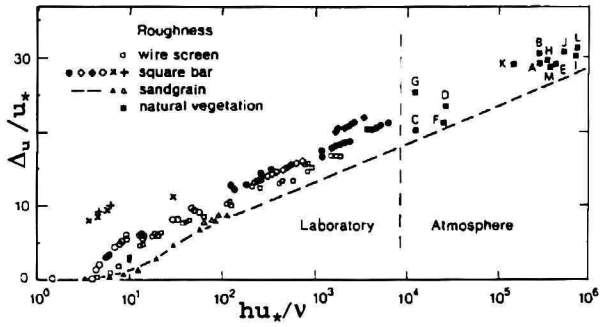

Fig. 5. The Δ_u/u_* as function of the roughness Reynolds number hu_*/ν (Raupach et al., 1991).

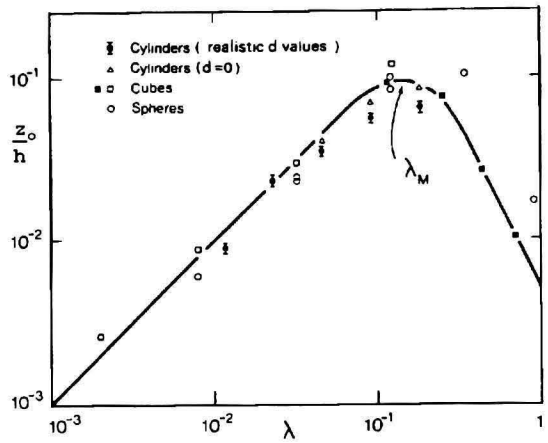

Fig. 6. The scaled roughness length z_0/h as function of λ (Raupach et al., 1991).

increases continuously as a function of hu_*/ν and for large values it can be described very well by a logarithmic function, i.e. $\Delta_u/u_* = k^{-1}\ln(hu_*/\nu) + B$ where B is a constant. At the very high Reynolds numbers that occur in the atmosphere, one may assume that Reynolds similarity applies so that all dependence of (u) on Reynolds number should disappear. This explains for instance the logarithmic dependence which we noticed above for Δ_u/u_*. Moreover, for these so-called fully rough flow conditions Reynolds similarity implies that the u_*z_o/ν must become proportional to hu_*/ν so that $z_o/h = f(\lambda)$. This relationship is illustrated in Fig. 6. It shows that for small values of λ the z_0/h increase linearly with λ until a maximum value is reached. Beyond the value of λ where the maximum occurs, the z_o/h decreases again which is attributed to the partial sheltering of the roughness elements when they are very densely packed on the surface.

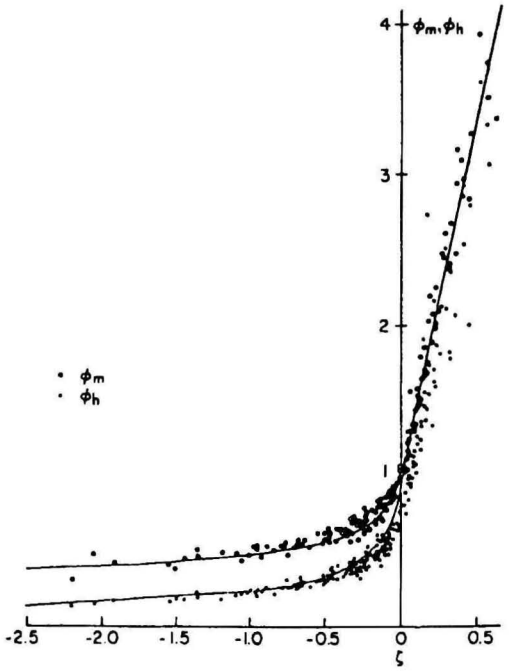

Fig. 7. The flux relationships ϕ_m and ϕ_h in the surface layer scaled according to Monin-Obukhov similarity where ζ stands for z/L; the lines denote empirical expressions such as discussed in the text and the symbols are observations (Fleagle and Businger, 1980).

3.2 Diabatic surface layer

Including the effects of buoyancy implies that we should include the Monin-Obukhov length L (equation 2) in the scaling parameters introduced in section 3.1. Our hypothesis is that these parameters are sufficient to scale the velocity profile in the surface in terms of a universal function. This is called Monin-Obukhov similarity. Monin-Obukhov similarity leads to the following expressions for the gradient of the mean velocity and temperature:

$$\frac{kz}{u_*}\frac{\partial u}{\partial z} = \phi_m\left(\frac{z}{L}\right) \quad , \quad \frac{kz}{\theta_*}\frac{\partial \theta}{\partial z} = \phi_h\left(\frac{z}{L}\right) \, , \tag{9}$$

which are illustrated in Fig. 7. The ratio z/L can be interpreted as describing the influence of stability effects in the surface layer. When $z/L \approx 0$ stability effects can be neglected and in view of (6) this implies that $\phi_m(0) = 1$. We see that this occurs for small values of z or for small values of $\overline{w'\theta'}_o$ with respect to u_*. In other words stability effects have only effect at sufficient large values

of z. For a detailed discussion of these so-called flux-profile relationships we refer to the literature mentioned in the introduction.

Here we draw attention to the comparison of (9) with engineering data in particular the data taken at conditions of free convection that is $-z/L \to \infty$. Atmospheric measurements suggest that in this limiting case the velocity and temperature gradient behave as

$$\phi_m\left(\frac{z}{L}\right) \simeq \left(-\frac{z}{L}\right)^{-1/4} \quad , \quad \phi_h\left(\frac{z}{L}\right) \simeq \left(-\frac{z}{L}\right)^{-1/2} \quad . \tag{10}$$

These results are directly in contradiction with the main assumption of free convection that the mean horizontal velocity should approach zero. Also the temperature gradient given by (10) differs from the engineering data for free convection above a horizontal surface. In the latter case one finds that $\partial\overline{\theta}/\partial z \simeq z^{-4/3}$ which implies $\phi_h \simeq (-z/L)^{-1/3}$ rather then the results given by (10). Although several attempts have been made to explain this anomalous behaviour of ϕ_h in the atmosphere with respect to the laboratory (see e.g. Yaglom, 1994), the problem remains largely unresolved.

4 Surface-layer Turbulence

4.1 Neutral surface layer

The main assumption made in order to scale turbulence variables in the surface layer goes back to (Townsend, 1961) who states that at a sufficiently large distance from the surface, i.e. for $z/z_0 \gg 1$, turbulence can be assumed to be in local equilibrium. Local equilibrium means here that the production and dissipation processes of turbulence are at a given height z in balance. As a result only the u_* and z remain as scaling parameters.

This local equilibrium hypothesis is in agreement with the logarithmic profile introduced by matching arguments in 3.1. Namely, for the production of turbulence the local equilibrium scaling provides in neutral conditions

$$-\overline{u'w'}\,\frac{\partial u}{\partial z} = \frac{u_*^3}{kz} \ ,$$

which together with $-\overline{u'w'} \simeq u_*^2$ in the surface layer leads to a logarithmic profile.

For turbulence statistics such as the variances of the velocity fluctuations the equilibrium scaling in the neutral surface layer would imply that these variances should become equal to a universal constant. Although this

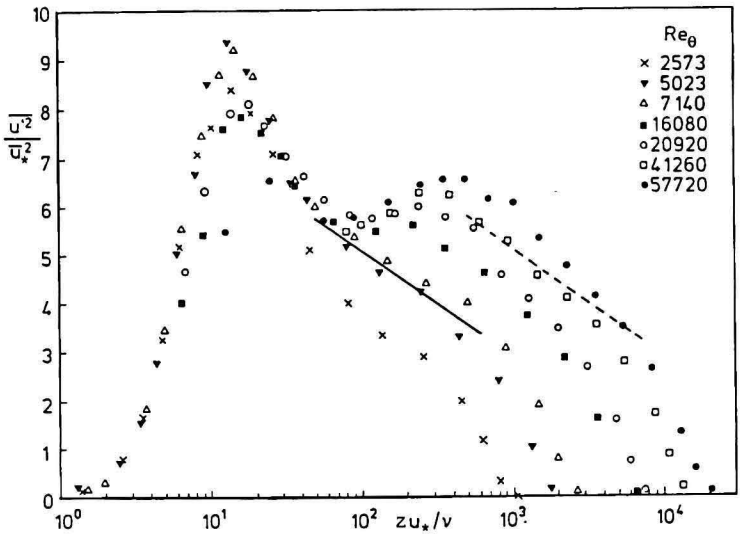

Fig. 8. Standard deviation of the velocity fluctuations in direction along the mean velocity scaled with u_* at various values of the Reynolds number (Fernholtz and Finley, 1996).

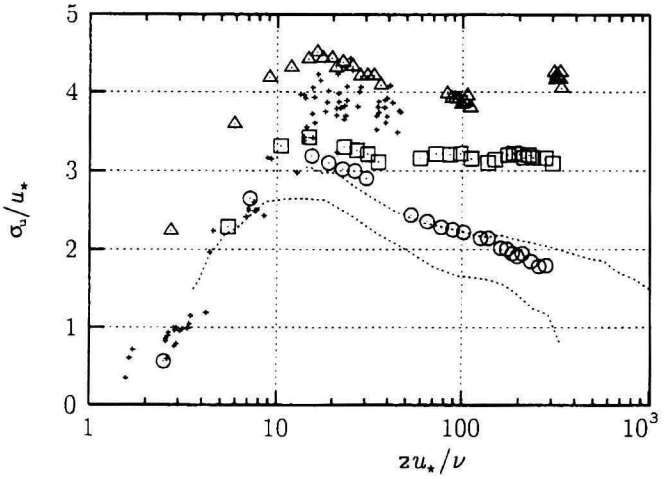

Fig. 9. Horizontal velocity variance in direction along the mean velocity as a function of scaled height above a smooth surface in the neutral atmospheric surface layer (Folz, 1997).

result has been long considered as controversial, recent laboratory data shown in Figures 8 seem indeed to show that at high values of the Reynolds number there is a region where the velocity fluctuations when scaled with u_* become constant as a function of height. In the atmosphere careful measurement of the dependence of the velocity fluctuations with height in the neutral surface layer are very scarce. In (Folz, 1997) some atmospheric data taken above a smooth surface are reported and they are shown in Fig. 9. The data shown

in this figure show a reasonably constant value σ_u/u_* as function of zu_*/ν for individual experiments. However, there is a large scatter in the actual values between the different experiments. Moreover, the values are on the average larger than those obtained in the laboratory which can be partly attributed to effects of stability.

In (Panofsky and Dutton, 1984) results are reported for the average value of the standard deviation of the velocity fluctuations in the neutral surface layer over flat grass land. These are: $\sigma_u/u_* = 2.39 \pm 0.03$, $\sigma_v/u_* = 1.92 \pm 0.05$ and $\sigma_w/u_* = 1.25 \pm 0.03$. For σ_u , the values are in reasonable agreement with the laboratory data shown above.

There is an additional difficulty when scaling the velocity variance. This was first pointed out by (Bradshaw, 1967) who argued that the turbulence motions which contribute to the velocity variance, should be distinguished into active and inactive motions. These are the turbulent motions which are responsible for the vertical flux of momentum, and the motions which are driven by large-scale eddies in the boundary layer respectively. The latter motions do not contribute to momentum transport in the surface layer. Consequently, the active motions can be scaled following the equilibrium hypothesis introduced above but the inactive motions depend rather on the boundary-layer height. In particular the horizontal velocity fluctuations are assumed to be influenced by these inactive motions. This fact would imply that the value of the horizontal velocity variance is strongly dependent on the type of flow that one considers and also on other parameters that influence the large scale motions within the boundary layer such as the boundary-layer height.

Mociuzuki and Nieuwstadt (1996) provide experimental data on the maximum value of σ_u/u_* as collected for various flow geometries. For all geometries and for a large range of Reynolds number the value 2.7 was found for this maximum value. This seem to be also in agree with the maximum values of the profiles shown in Fig. 8 and also in reasonable agreement with the average values for the atmosphere as quoted above. This fact contradicts a large contribution by inactive motions because in that case the maximum value of σ_u/u_* would depend on flow geometry and also on Reynolds number based on the boundary-layer height. Therefore, one should conclude that the distinction into active and inactive motion when considering horizontal velocity fluctuations is not resolved.

4.2 Diabatic surface layer

The local equilibrium hypothesis introduced above can be also applied in this case. However, we have to allow for the influence of buoyancy. This can be accounted for when we add the Obukhov length L to the scaling parameters. The resulting scaling which again is known as Monin-Obukhov scaling, then leads to the following expressions for the standard deviation of the vertical

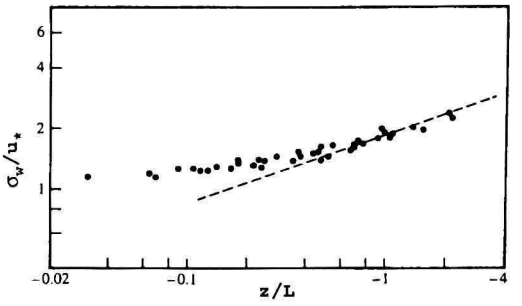

Fig. 10. The standard deviation of the vertical velocity fluctuations as function of z/L according to Monin-Obukhov similarity for unstable conditions, i.e. $L < 0$; the dashed lines are the expression for free convection discussed in the text; the symbols denote experiments (Wyngaard et al., 1971).

velocity and temperature fluctuations:

$$\frac{\sigma_w}{u_*} = f_w\left(\frac{z}{L}\right) \quad , \quad \frac{\sigma_\theta}{\theta_*} = f_\theta\left(\frac{z}{L}\right) \; . \tag{11}$$

These relationships are compared with atmospheric data in Fig. 10 for the case of the unstable surface layer. We find that the data plot excellently on a single curve which can be considered as confirmation of Monin-Obukhov similarity. When $-L$ becomes very small, e.g. when $\overline{w'\theta'}_o$ becomes large, one would expect that above certain height the u_* does not play a role any more. Alternatively, one could argue that in this case the turbulence is dominated by buoyancy production and the u_* is no longer a relevant scaling parameter. The only scaling parameters that remain are z and L and the only possibility to satisfy this constraint is when the scaling relations (11) reduce to

$$\frac{\sigma_w}{u_*} \simeq \left(\frac{z}{L}\right)^{1/3} \quad , \quad \frac{\sigma_\theta}{\theta_*} \simeq \left(\frac{z}{L}\right)^{-1/3} \; . \tag{12}$$

These expression are indicated in Fig. 10 for σ_w by the dashed line where for the proportionality constants we have used 1.8 . We find that for large values of $-z/L$ the data indeed follow the expressions given by (12).

The expressions (12) are known to be also valid in laboratory experiments under so-called free-convection conditions. One may point out here that it could be perhaps considered as surprising that the turbulence fluctuations follows the same free convection scaling both in the atmosphere and the laboratory whereas we have found in section 3.2 that this is not the case for the mean profiles.

5 Neutral boundary layer

In the following sections we consider the scaling of the atmospheric boundary layer above the surface layer which we shall indicate as the outer layer. The scaling of the outer layer is much less well developed than for the surface-layer. One of reasons is of course that it is much more difficult to obtain experimental data in the outer layer. An exception is the experimental data described by Grant (1992). Another reason is that in the outer layer the boundary-layer structure is sensitive to influence by other factors such as e.g. horizontal advection. These factors will introduce additional scaling parameters so that a simple scaling with only a few parameters is usually not possible for the outer layer.

Let us first consider the outer layer for the case of the neutral boundary layer. In engineering this case has been extensively studied. It has been established that the outer-layer velocity profile can be described by a so-called defect law of the form

$$\frac{U_e - u}{u_*} = F\left(\frac{z}{\delta}\right) , \tag{13}$$

where U_e is again the velocity at the edge of the boundary layer. In general one assumes that in the atmospheric boundary layer a similar form as the defect law is valid. However, there is no convincing experimental evidence for this. The reason is apart from the arguments mentioned above, also due to the fact that a neutral boundary layer is hardly observed in the atmosphere. In almost all cases the influence of temperature fluctuations is non-negligible. To show this we introduce the Richardson number defined as

$$Ri' = \frac{g}{T_o}\frac{\theta'\,\delta}{u_*^2} ,$$

which gives the ratio of the acceleration due to a temperature fluctuation θ' with respect to the turbulent acceleration u_*^2/δ. We assume that for $Ri' < 0.1$ buoyancy effects can be neglected. If we take $\delta = 500$ m, $g/T_o = 0.03$ m °K/s and $u_* = 0.3$ m/s, we find that this condition is only satisfied for $\theta' < 6\,10^{-4}$ °K. We must therefore conclude that even small temperature fluctuations quickly lead to appearance of buoyancy effects in the boundary layer.

Therefore, our information on the neutral atmospheric boundary layer comes mostly from numerical simulations. Examples are the large-eddy simulations described in Mason and Thomson (1987) and Andren et al. (1994). These studies confirm that the velocity profile in the neutral atmospheric boundary layer can be described by the defect law (13) which shows that in the outer layer the velocity profile does not depend on surface characteristics such as z_o. This forms the basis for the matching procedure which leads to the

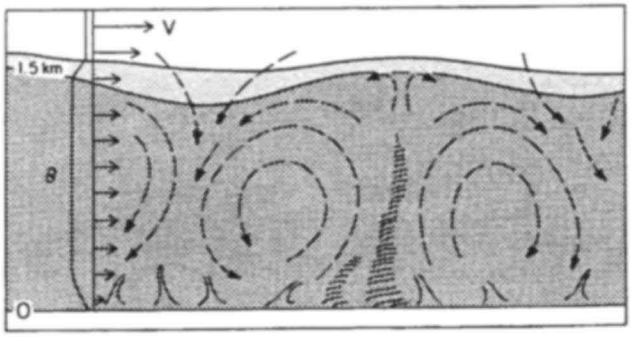

Fig. 11. Schematic picture of the convective boundary layer (Wyngaard, 1992).

logarithmic profile (6).

With respect to the turbulence statistics one may take the same approach, i.e. they are assumed to scale in terms of u_* and δ.

6 Convective boundary layer

In Figure 11 we show a schematic picture of the convective boundary layer, i.e. $\overline{w'\theta'}_o > 0$. We see that the turbulence structure is composed of large eddies which fill the whole boundary layer. These eddies are a direct result of buoyancy production. They consist mainly of air heated up at the surface and they are known as thermals or plumes. The influence of shear production can be neglected and this means that u_* plays no longer a role. Based on this consideration the scaling parameters for the convective boundary layer are: δ, w_* and z, where the so-called convective velocity scale is defined as

$$w_* = \left(\frac{g}{T_o} \, \overline{w'\theta'}_o \, \delta \right)^{\frac{1}{3}} . \tag{14}$$

As a result of the high turbulence intensity in the convective boundary layer mixing is intensive. Consequently mean variables, such as velocity and temperature, are well-mixed, i.e. their variation as a function of height is small.

The scaling of all turbulence variables in terms of the parameters given above is known as mixed-layer scaling. For instance for the standard deviation of the vertical and horizontal velocity fluctuations mixed-layer leads to the following expressions

$$\frac{\sigma_w}{w_*} = f_w\left(\frac{z}{\delta}\right) , \qquad \frac{\sigma_u}{w_*} = f_u\left(\frac{z}{\delta}\right) , \qquad \frac{\sigma_v}{w_*} = f_v\left(\frac{z}{\delta}\right) , \tag{15}$$

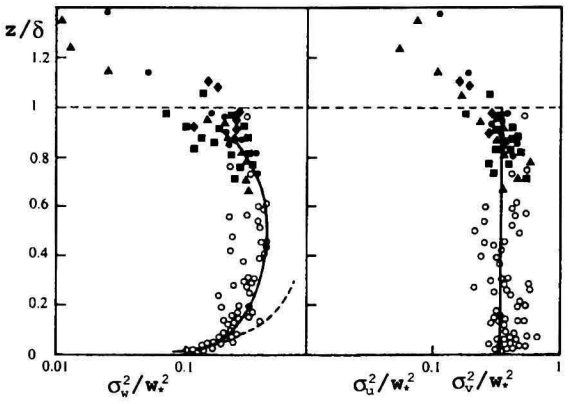

Fig. 12. Vertical profiles of the standard deviation of vertical velocity fluctuations (σ_w) and the horizontal velocity fluctuations (σ_u and σ_v) scaled following mixed layer scaling; the solid lines denote empirical fits to the observations indicated by the symbols and the dashed the result of matching to the surface-layer scaling (Garratt, 1992).

which are illustrated in Fig. 12. These results are a clear confirmation of mixed-layer scaling. Also laboratory experiments and numerical simulations give equally positive results. One may wonder whether the expressions (15) which are valid in the mixed-layer, can be matched to the expressions (11) that we have derived for the surface layer. Without going onto the details we find that matching leads to the following explicit profiles for the velocity and temperature fluctuations:

$$\frac{\sigma_{u,v,w}}{w_*} \simeq \left(\frac{z}{\delta}\right)^{1/3} , \qquad \frac{\sigma_\theta}{T_*} \simeq \left(\frac{z}{\delta}\right)^{-1/3} , \tag{16}$$

where the temperature scale T_* is defined as $T_* = \overline{w'\theta'}_o/w_*$. From Fig. 12 it is clear that the matching result (16) is followed by the vertical velocity fluctuations. In this case the matching result becomes equal to the free convection expression (10) that we have derived in the surface layer and which we can now interpret as matching between the surface layer and outer boundary layer. The same is true for the temperature fluctuations.

Matching seems to fail for the horizontal velocity fluctuations which according to Fig. 12 do not seem to follow an expression as given by (16). The explanation is that the horizontal fluctuations are primarily determined by the large-scale thermals which depend on the boundary-layer height and not on the distance to the surface. The consequence is that the horizontal velocity fluctuations near the surface do not scale with the height above the surface but rather with δ. This is the same argument as introduced in section 4.1 in terms of active and inactive motions.

The consequence is that the horizontal velocity fluctuations when ex-

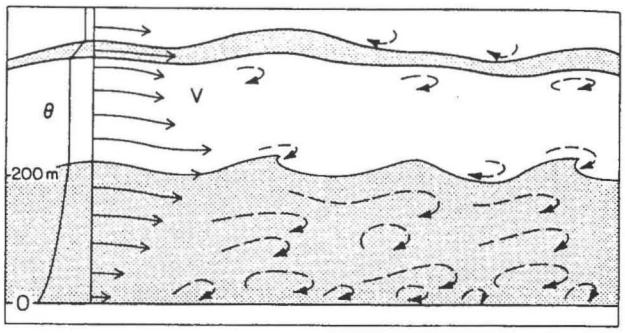

Fig. 13. Schematic picture of the stable boundary layer (Wyngaard, 1992).

pressed in terms of mixed-layer scaling should approach a constant for $z \rightarrow 0$ which according to the results plotted in Fig. 12 is equal to 0.6. Rewriting this result in terms of surface-layer variables we obtain

$$\frac{\sigma_{u.v}}{u_*} = 0.8 \left(-\frac{\delta}{L} \right)^{1/3} .$$

which clearly show that including inactive motions leads to a dependence of surface-layer variables on overall boundary-layer parameters such as δ.

7 Stable boundary layer

A schematic picture of the stable boundary layer is shown in Fig. 13. In comparison with the convective boundary layer illustrated in Fig. 11, we observe that the structure of the stable boundary layer is completely different. Most noticeable is the fact that the stable boundary layer is rather shallow and that there are no motions which extend from the surface to the top of the boundary layer. The latter result is the consequence of the stability by which vertical motion in a stable boundary layer is opposed. Turbulent eddies will thus be small so that their length scale $\ell \ll \delta$.

In a stable boundary layer only shear production remains as a source of turbulence and it will be clear that turbulence should be scaled in terms of this process. However, the correct scaling velocity is not the surface friction velocity u_*. Because of the fact that $\ell \ll \delta$, turbulence at each height z will be only determined by local processes. In other words production depends only on local shear and turbulence feels the influence of the surface only indirectly. As a result the appropriate scaling parameters are : $\overline{w'\theta'}$, τ and z, where $\overline{w'\theta'}$ and τ stand for the turbulent temperature and momentum fluxes at some height z above the surface. With these parameters and the buoyancy parameter g/T_o

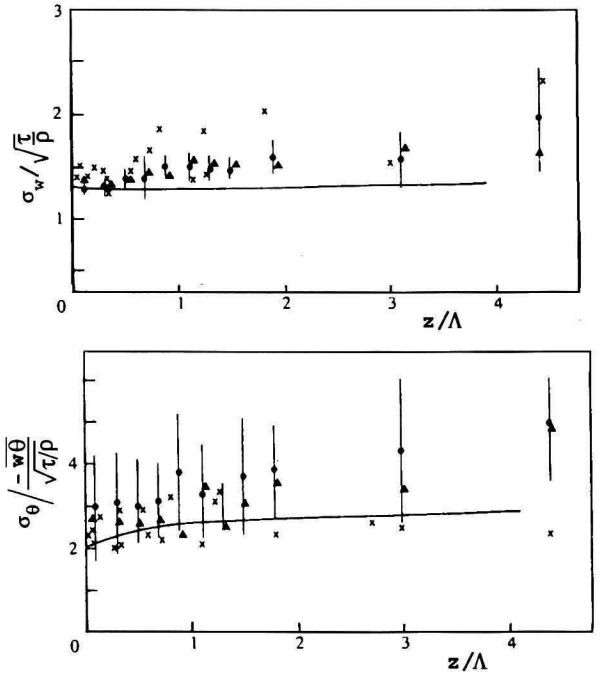

Fig. 14. Local scaling applied to the standard deviation of the vertical velocity fluctuations (σ_w) (above) and the temperature fluctuations (σ_θ) (below); the solid line is second-order turbulence model; each symbol denotes the average over several observations and the vertical lines given the variation among these observations (Nieuwstadt, 1984).

we can define a length scale

$$\Lambda = -\frac{(\tau/\rho)^{3/2}}{k\frac{g}{T_o}\overline{w\theta}} , \tag{17}$$

which is known as the local Monin-Obukhov length. Scaling in terms of the parameters mentioned above is known as local scaling (Nieuwstadt, 1984). We note that local scaling resembles the Monin-Obukhov similarity of the surface layer discussed in section 3 in which u_* and L are used as scaling parameters. As a consequence local scaling matches automatically to Monin-Obukhov similarity when $z \rightarrow 0$.

Application of local scaling to the standard deviation of the vertical velocity and of the temperature fluctuations leads to

$$\frac{\sigma_w}{\sqrt{\tau/\rho}} = f_w\left(\frac{z}{\Lambda}\right) , \qquad \frac{\sigma_\theta}{\overline{w\theta}/\sqrt{\tau/\rho}} = f_\theta\left(\frac{z}{\Lambda}\right) \tag{18}$$

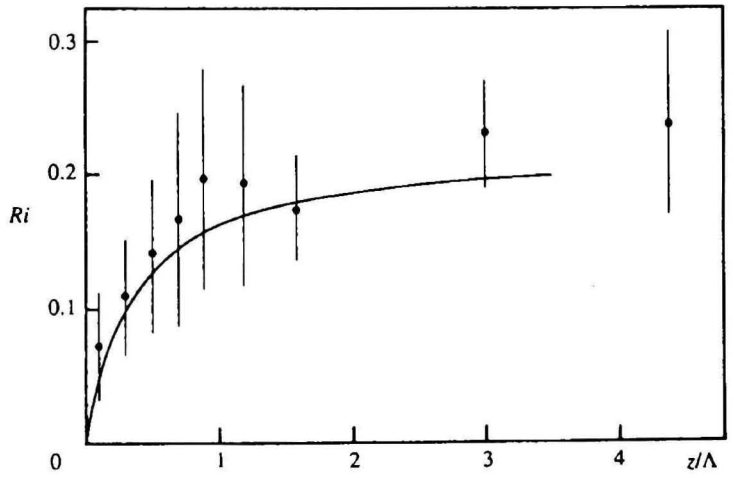

Fig. 15. The local scaling of the Richardson number Ri; the solid line is second-order turbulence model; each symbol denotes the average over several observations and the vertical lines given the variation among these observations (Nieuwstadt, 1984).

These expressions are compared with observations in Fig. 14. Taking into account the large scatter which is unavoidable for measurements in stable atmospheric conditions, we find reasonable confirmation for our local scaling approach. Another parameter to which we may apply local scaling is the so-called gradient Richardson number Ri defined as

$$Ri = \frac{\dfrac{g}{T_o}\dfrac{\partial\theta}{\partial z}}{\left(\dfrac{\partial u}{\partial z}\right)^2 + \left(\dfrac{\partial v}{\partial z}\right)^2} \,. \tag{19}$$

The Ri can be interpreted as a measure of stability. According to local scaling Ri must be only a function of z/Λ. We find in Fig 15 that on the average the data of Ri plot reasonable well on a single curve which is again a confirmation of local stability.

We note that the curve in Fig. 15 approaches a constant value for $z/\Lambda \to \infty$ which we denote as the critical Richardson number Ri_{cr}. This is characteristic for another scaling regime in the stable boundary layer which is generally called z-less scaling (see Fig 1.). The background is that at large heights in the stable boundary layer, i.e. $z/\Lambda \to \infty$, local turbulence conditions are completely decoupled from direct influence of the surface. As a consequence the height z should drop from the list of scaling parameters introduced above. It implies that all locally scaled variables (such as the Richardson number) should approach a constant value in this limit.

Apart from the turbulence statistics we can also consider the behaviour of the mean profiles in the stable boundary layer. Scaling relationships can

only be found for the case of the stationary boundary layer and for further discussion we refer to (Nieuwstadt, 1984) .

Apart from the experimental validation as mentioned above, the results of local scaling have been also confirmed by numerical simulation (Mason and Derbyshire, 1990) . Moreover in (Derbyshire, 1990) the theory of local scaling has been extended and it is shown that this theory implies that in a continuous turbulent boundary layer the surface temperature fluxes bound from above by

$$\frac{g}{T_o}\,\overline{w'\theta'}_o \leq \frac{Ri_f}{\sqrt{3}} G^2 f \ .$$

Here Ri_f is the flux Richardson number which for the case of z-less scaling is proportional to Ri. Furthermore G is the geostrophic wind speed and f is the Coriolis parameter. The explanation for this perhaps surprising result is that in stable conditions (in combination with rotation) there is a limit to the downward temperature flux that turbulence can support.

Finally, we want to mention here the study reported by (Schumann and Gerz, 1995) where an extension to local scaling is proposed. The point of departure is the quasi-stationary kinetic energy budget of turbulence which can be written as

$$0 = P + B + T - \epsilon \ . \tag{20}$$

Here P is the shear production which is always larger than zero, B is the buoyant production which in a stable boundary layer is smaller than zero, and ϵ is the viscous dissipation. T is the transport term. In complete local equilibrium T is zero by definition , but it is argued in (Schumann and Gerz, 1995) that even a small value of T may have a non-negligible effect.

The ratio between the energy production to the energy destruction can be defined as $G = P/(\epsilon - B)$. With the help of G the budget (20) can then be written as $T = (1 - G)(\epsilon - B)$, which shows that for $G = 1$ the condition of local equilibrium is retrieved for which we have argued above that in the limit of z-less scaling $Ri = Ri_{cr}$. Next the G is parameterized as

$$G = G_o^{1-Ri/Ri_{cr}} \ , \tag{21}$$

which satisfies local equilibrium for $Ri = Ri_{cr}$. The G_o can be interpreted as the ratio between shear production and viscous dissipation at neutral conditions and it should be larger than 1 according to Schumann and Gerz. This implies that $T < 0$ for $Ri < Ri_{cr}$ and $T > 0$ for $Ri > Ri_{cr}$ which means energy transport from regions with $Ri < Ri_{cr}$ to regions with $Ri > Ri_{cr}$. Their arguments allow extension of the theory of local scaling to stronger stability beyond $Ri = Ri_{cr}$. A comparison is made by (Schumann and Gerz, 1995) of this theory both with atmospheric and engineering data. The agreement is

satisfactory and this shows that the effect of stable conditions in engineering and atmospheric flows can be described within the same theoretical frame work.

8 Final Remarks

Based on identification of the physical processes that determine turbulence, we have reviewed scaling hypotheses. To identify the dominating processes, the boundary layer has been subdivided in so-called prototypes which are based on the effects of stability in the boundary layer. With the scaling results we are able to describe the structure of each prototype of the atmospheric boundary layer in detail (see Fig. 11). Moreover, we find that the scaling results compare in general well with equivalent results obtained for engineering flow where it should be noted that in engineering flow influence of stability is usually not as important. However, the fact that the atmospheric and engineering data are consistent when properly scaled, implies that the scaling results based on engineering flow at low to moderate Reynolds numbers remain valid up to very large Reynolds numbers.